



KRITIKA SUMMER PROJECTS 2023

Exploring the Radio Sky

Darsh Ambade

KRITTIKA SUMMER PROJECTS 2023

Exploring the Radio Sky

Darsh Ambade¹

¹Indian Institute of Science Education and Research, Mohali

Abstract

Radio astronomy has revolutionized our understanding of the Universe by probing celestial objects and phenomena by observing radio waves. This project report focuses on acquiring and analyzing radio astronomy data using prominent telescopes such as the Very Large Array (VLA) and the Giant Metrewave Radio Telescope (GMRT). The project begins with an introduction to radio astronomy, providing a comprehensive overview of the principles and techniques involved. It covers the basics of radio wave propagation, instrumental components, and observational methods employed in the field. Additionally, the report delves into the significance of the 21cm line, a spectral line emitted by neutral hydrogen atoms, GW170817 a revolution in multi-messenger astronomy and Fast Radio Bursts.



Contents

1	Introduction to the Radio Sky	5
1.1	A Quick Overview	5
1.2	Equatorial Coordinate System	5
1.2.1	Right Ascension and Declination	6
1.2.2	Observer-Centered Definitions	6
2	Observational Basics	9
2.1	Single Dish Observations	9
2.1.1	Measurement of Antenna Temperature	10
2.1.2	Beam Pattern and Angular Resolution	10
2.2	Aperture-Synthesis	11
2.2.1	Two Element Interferometer	11
3	Fundamentals to Radiation Physics	13
3.1	Measuring amount of Radiation	13
3.1.1	Luminosity	13
3.1.2	Flux and Flux Density	13
3.2	21cm Hydrogen Line	14
3.2.1	*Activity : Galaxy Rotation Curve	14
4	Exploring and Analysing	17
4.0.1	Extracting and Working with Radio Telescope data	17
4.0.2	* Activity : CMB - a near perfect black body	18

4.1	CASA (Common Astronomy Software Applications)	19
4.2	GW170817: Merging Neutron Stars and the Dawn of Multi-Messenger Astronomy	21
4.3	Fast Radio Bursts: Analysing Pulsar and its Dispersion Measure	23



1. Introduction to the Radio Sky

1.1 A Quick Overview

Electromagnetic (EM) waves are a form of energy propagation that do not require a medium to travel through. They consist of electric and magnetic fields oscillating perpendicular to each other and to the direction of wave propagation. EM waves encompass a wide range of frequencies, collectively known as the electromagnetic spectrum, which includes radio waves, microwaves, infrared, visible light, ultraviolet, X-rays, and gamma rays.

Radio waves are a type of electromagnetic wave used in radio astronomy. Radio telescopes capture and analyze radio waves emitted by celestial objects such as stars, galaxies, and pulsars. By studying these radio emissions, astronomers gain insights into the composition, structure, and behavior of the universe. Radio astronomy has provided significant discoveries, including the detection of cosmic microwave background radiation, pulsars, and distant galaxies, expanding our understanding of the cosmos.

1.2 Equatorial Coordinate System

The equatorial system is a celestial coordinate system commonly used in astronomy to locate celestial objects on the celestial sphere. It provides a consistent reference frame that remains fixed with respect to the stars, allowing astronomers to accurately determine the positions of objects regardless of Earth's rotation.

The celestial sphere is imagined as an extension of Earth's equatorial plane into space in the equatorial system. It is divided into two primary components: the celestial equator and the celestial poles. The celestial equator is an imaginary circle around the celestial sphere directly above Earth's

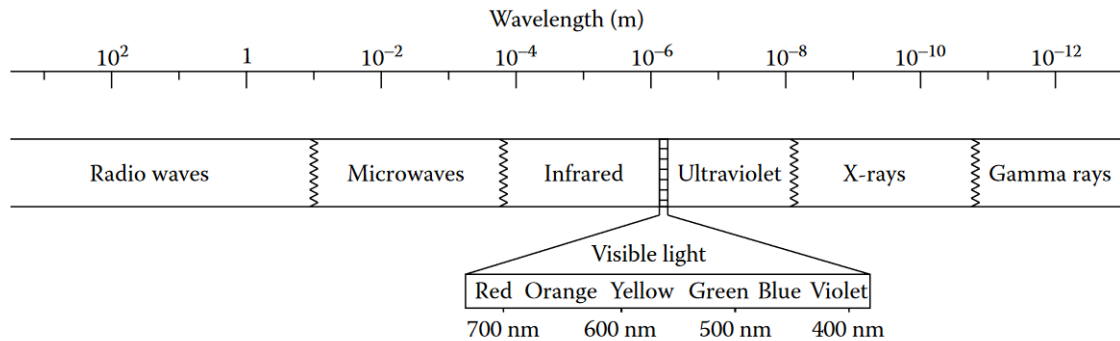


Figure 1.1: Electromagnetic Spectrum (6)

equator. It divides the celestial sphere into two halves, the northern and southern celestial hemispheres.

1.2.1 Right Ascension and Declination

RA (Right Ascension) and DEC (Declination) are the two fundamental properties of measuring the position of an object in the sky. Declination is the angular distance measured to the north or south of the celestial sphere. A very good analog to DEC is latitude in the celestial coordinates. DEC is measured in degrees, minutes, seconds and is conventionally positive for the north and negative for the southern part of the celestial sphere.

While defining RA (Right Ascension), it is essential to note that the definition should be with respect to the celestial sphere and not the Earth. It should also be noted that the angular separation of any two lines is not the same for one latitude. To be precise, the angular separation of two RA lines is proportional to the cosine of DEC. At the equator, as there are 24 hours of RA, 1 h of RA = 15 degrees of arc, so 1min of RA = 15 min of arc, and so on

$$\text{Seconds of arc} = 15 \cos(\delta) * \text{seconds of RA}$$

where, δ is DEC

1.2.2 Observer-Centered Definitions

1. Horizon : This delineates the extent to which specific portions of the sky are observable at a given time. This limitation arises from terrestrial obstacles, such as the Earth's surface and man-made structures, obstructing our view of the sky. In a hypothetical scenario where Earth was transparent, it would be possible to observe the sky beneath our feet by looking through the Earth. However, due to Earth's non-transparency, this portion of the sky remains hidden from our view, lying beyond our visual horizon.

2. Zenith : The celestial point directly above an observer. As the sky undergoes continuous rotation, this zenith point on the celestial sphere constantly

shifts unless one is situated at either the North or South Pole, where it remains fixed.

3. Altitude or elevation : These are different terms used to describe the vertical angle of an object above the observer's horizon at a specific moment. This angle is referred to as "altitude" or "elevation." For instance, when a star is positioned at the horizon, either during its rising or setting, its altitude or elevation is 0°. On the other hand, when the star is directly overhead, at the zenith, its altitude or elevation reaches 90°. It's important to note that this measurement represents an angle, not a physical distance.

4. Azimuth : This refers to the angular position that is perpendicular to the altitude and is used to define the object's location along the horizon with respect to due north. When an object is situated to the north of the zenith, its azimuth is measured as 0°. Conversely, if the object is positioned to the south of the zenith, its azimuth is 180°. An azimuth of +90° corresponds to due east, while an azimuth of 270° corresponds to due west. It is essential to understand that both azimuth and altitude together form a pair of angles that fully describe an object's position in the sky relative to the observer. This detail is significant as all observers will perceive the same Right Ascension (RA) and Declination (Dec) values for an astronomical object. However, the altitude and azimuth of the object will differ for observers at various locations and even for the same observer at different times of the day.

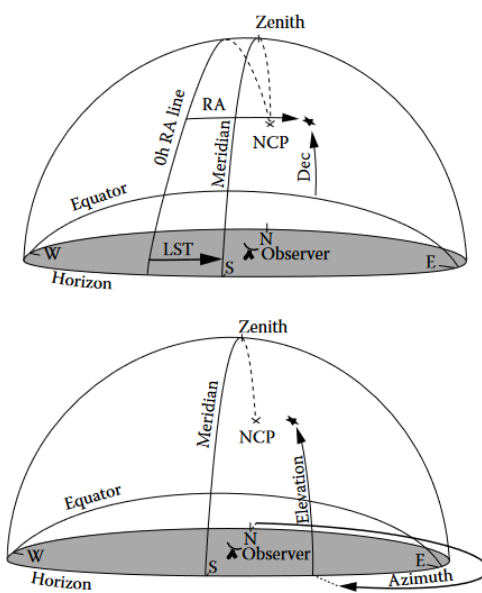


Figure 1.2: Depiction of sky coordinates as viewed by the observer (top) and observer-centered coordinates (bottom). (6)

5. Meridian : It is an imaginary line that extends from the north celestial pole, passes through the observer's zenith, and reaches the south celestial

pole. Essentially, it is the line of Right Ascension (RA) that runs through the point directly above the observer.

6. Hour angle (HA) : Hour Angle (HA) is the amount of time (measured in hours) that has passed since the object crossed the observer's meridian, also known as the time of transit.

7. Local sidereal time (LST) : This is defined as the RA of the meridian.

$$HA = LST - RA$$



2. Observational Basics

2.1 Single Dish Observations

A Single Dish antenna detects the power emanating from the point source. However, it is evident that the power registered by the telescope is not solely attributed to the source. To ascertain the specific amount of power originating solely from the astronomical source, one needs to subtract the power contributed by receiver noise and other undesirable radiation sources. This forms the core principle of Single-dish radio observations and is accomplished through Switched Observations. The power detected from a source due to radiation can be expressed as follows:

$$P = F_\nu A_{eff} \Delta v$$

Radio astronomers usually express the power measured from an astronomical source by its equivalent temperature called antenna temperature (T_A), while the noise power produced by the telescope receiver components is referred to as the noise temperature (T_N). We lump all of the unwanted power together, and call it the system temperature (T_{sys}).

$$V_{on} = \alpha G k \Delta v (T_A + T_{sys})$$

where,

V_{on} is the Voltage when pointed at the source α is the responsivity of the detector (and has units of V/W)

G is the dimensionless total receiver gain

k is Boltzmann's constant

$\Delta\nu$ is the observing bandwidth (set by the bandpass filter)

$$V_{off} = \alpha G k \Delta\nu T_{sys}$$

where,

V_{off} is the Voltage when pointed off source

Thus now we get,

$$V_{on} - V_{off} = \alpha G k \Delta\nu T_A$$

which is independent of the noise. So to find T_A , one then only needs to determine the conversion between temperature and voltage. Instead of substituting in all the factors involved ($\alpha G k \Delta\nu$), this is accomplished by a calibration of the system temperature, Which I wouldn't go into detail about here.

It is important to note that the total gain G varies over time and can cause significant deviations in the conversion of power to volts. To prevent this, the on and off observations are both made regularly throughout the observation. This technique is called as **Dicke Switching**.

2.1.1 Measurement of Antenna Temperature

The conversion between T_{sys} and V_{off} enables the calculation of the antenna temperature.

$$T_A = \frac{V_{on} - V_{off}}{V_{off}} T_{sys}$$

And, the uncertainty of T_A would be given as

$$\sigma(T_A) = \frac{T_{sys}}{\sqrt{\Delta t \Delta \nu}}$$

It should be noted that the above equation does not take variations and uncertainties like total gain G into account.

2.1.2 Beam Pattern and Angular Resolution

The sensitivity of a telescope as a function of angle relative to the pointing direction is known as the telescope's beam pattern, or power pattern, (See Figure 2.1) and is a fundamental characteristic of the telescope.

The standard convention for defining angular resolution involves measuring the Full Width at Half Maximum (FWHM) of the main beam produced by the telescope. The optimal angular resolution is achieved when the primary reflector is uniformly illuminated, ensuring that the detector exhibits equal sensitivity to radiation reflected from all sections of the dish.

In this scenario, the FWHM of the main beam is calculated as follows:

$$\theta_{FWHM} = 1.02\lambda/D$$

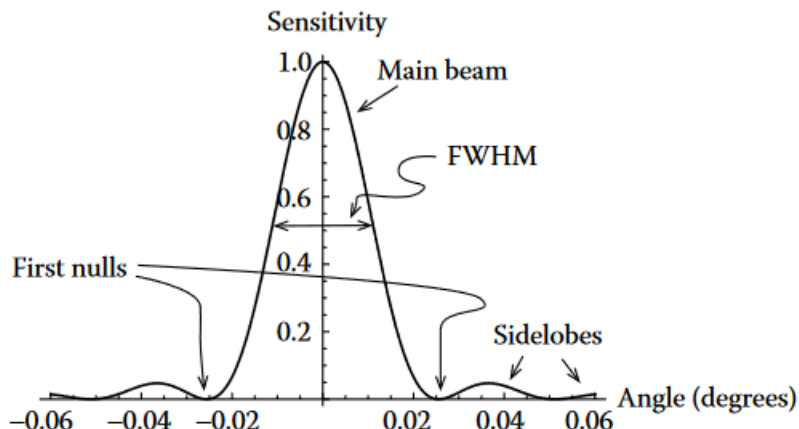


Figure 2.1: Sensitivity function, in one dimension for a 1.4-cm observation with a 40-m diameter radio telescope and 10-dB edge taper.(6)

In practice, a radio telescope does not usually have uniform illumination of the primary reflector due to the diffraction that occurs at the feed horn. The center of the reflector is more effective at collecting power than the edge. The ratio of the relative collecting ability per unit area between the edge and the center is called the edge taper and is usually expressed in decibels. For the optimum edge taper,

$$\theta_{FWHM} = 1.15\lambda/D$$

2.2 Aperture-Synthesis

Aperture Synthesis employs an array of numerous telescopes to generate high-resolution images. The primary benefit of this technique lies in its enhanced angular resolution. Radio astronomy's long wavelengths restrict single-dish observations, resulting in notably low resolution. However, this limitation is overcome by radio astronomers through the combination of several regular-sized radio telescopes in an array. By treating each telescope pair as an interferometer, a virtual telescope with an exceedingly large diameter can be effectively synthesized.

2.2.1 Two Element Interferometer

The basic unit of an aperture synthesis telescope is the two-element interferometer (Figure 2.2), composed of two antennas separated by a well-known distance with a well-known orientation.

The signals are calculated in two ways, either additively or multiplicatively average in time, both of which result in nearly the same results.

The electric field at the two antennas are,

$$E_1 = E_0 \cos(2\pi vt)$$

$$E_2 = E_0 \cos(2\pi v(t + \tau))$$

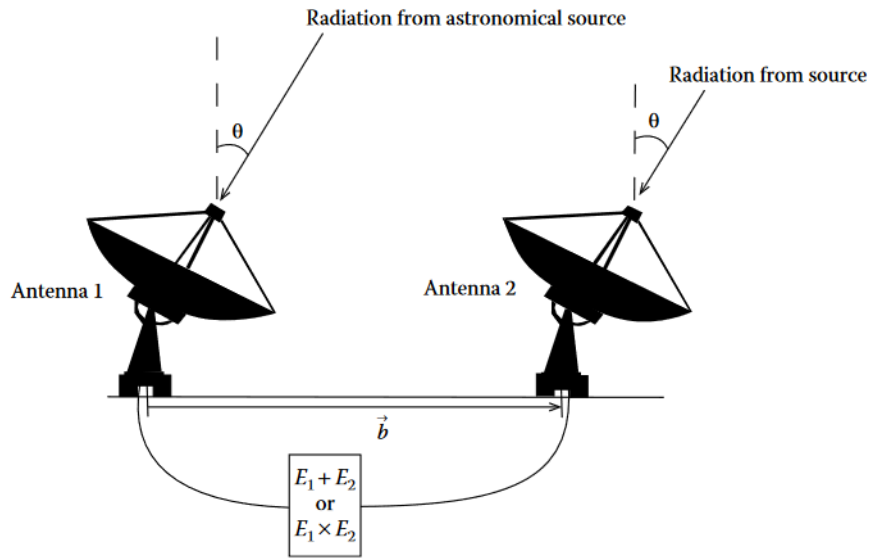


Figure 2.2: An interferometer, composed of two antennas separated by a distance b , receives signals from a radio source at an angle θ relative to the zenith.(6)

where the time delay τ can be calculated as,

$$\tau = \frac{\Delta s}{c} = \frac{b \sin \theta}{c} = \frac{b \sin \theta}{\lambda v}$$

Hence, the additive interferometer response would be

$$\langle (E_1 + E_2)^2 \rangle = E_0^2 \left[1 + \cos \left(2\pi \frac{b}{\lambda} \sin \theta \right) \right]$$

And the multiplicative response for the signal from interferometer would be,

$$\langle E_1 \cdot E_2 \rangle = \frac{E_0^2}{2} \cos \left(2\pi \frac{b}{\lambda} \sin \theta \right)$$

3. Fundamentals to Radiation Physics

3.1 Measuring amount of Radiation

3.1.1 Luminosity

Luminosity in radio astronomy refers to the total amount of energy radiated by a celestial object in the form of radio waves per unit of time. It is a fundamental property used to quantify the intrinsic brightness and power output of the source. The symbol L denotes luminosity and is typically measured in units of watts (W) or solar luminosities (L_\odot).

In radio astronomy, the luminosity of a source can be calculated by combining the observed radio flux density (F) with the distance (D) to the source. The formula gives the relationship between luminosity and flux density:

$$L = 4\pi D^2 F$$

where π is a mathematical constant (approximately 3.14159) and D is the distance to the source. This formula takes into account the spreading of the emitted radiation over an expanding sphere with the distance from the source.

3.1.2 Flux and Flux Density

Flux refers to the total energy received per unit of time from a celestial source across all wavelengths. It represents the overall brightness of the source and is commonly measured in units of watts per square meter (W/m^2). Flux provides information about the total power emitted by the source, but it does not consider energy distribution across different frequencies.

Flux density, however, refers to the energy received per unit of time from a celestial source at a specific frequency or wavelength. It measures the local power per unit area and is often expressed in watts per square meter

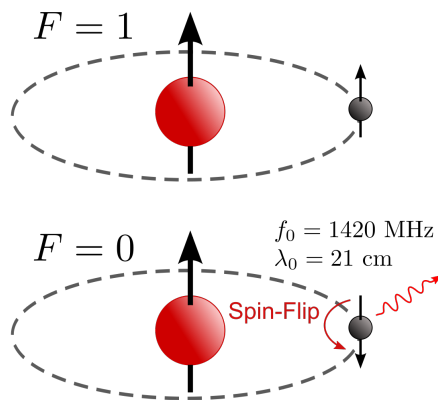


Figure 3.1: Electron Spin Flip resulting in the hydrogen 21cm line.(14)

per Hertz ($\text{W/m}^2/\text{Hz}$). Flux density provides information about the spectral distribution of energy, indicating how the source's brightness varies across different frequencies.

3.2 21cm Hydrogen Line

The 21cm hydrogen line, also known as the "21cm line" or the "hydrogen line," is a spectral line in the electromagnetic spectrum emitted by neutral hydrogen atoms. It arises from the transition between two energy levels in the hydrogen atom, which occurs when the spins of the electron and the proton flip. The wavelength of the 21cm line is approximately 21 centimeters, falling within the radio frequency range, which makes it easily detectable by radio telescopes.

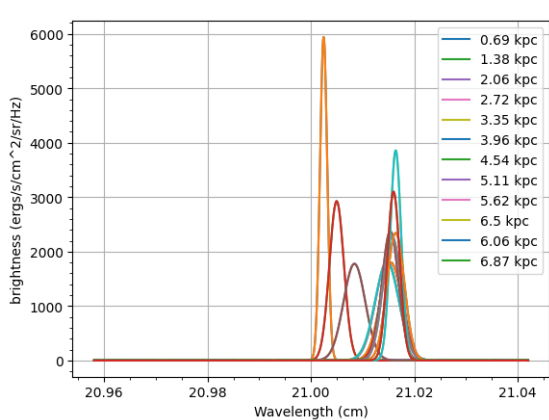
The significance of the 21cm line in radio astronomy is immense. Firstly, hydrogen is the most abundant element in the universe, and the 21cm line is directly associated with it. This makes it a powerful tool for studying a wide range of astrophysical phenomena.

In summary, the 21cm hydrogen line is a crucial tool in radio astronomy with profound significance. Its association with hydrogen, abundance in the universe, redshifted nature, and cosmological implications make it invaluable for studying the formation and evolution of galaxies, probing the large-scale structure of the universe, exploring the early universe, and facilitating practical aspects of radio astronomy.

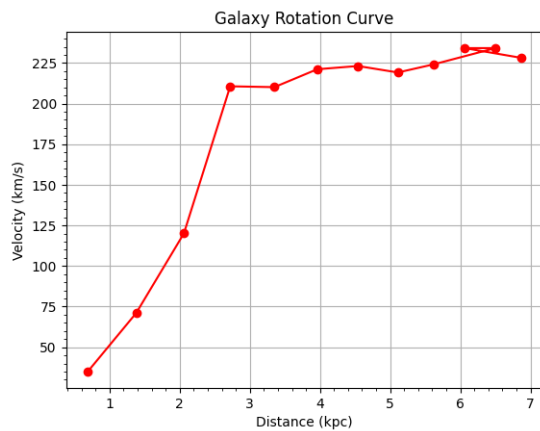
3.2.1 *Activity : Galaxy Rotation Curve

For this activity a synthetic spectral data (13) was created. From this data we will try to plot a Galaxy Rotation Curve which is the plot of velocity v/s distance of stars in that Galaxy. The above data contains various files at different distances in the 21cm Hydrogen line when plotted all together we get the plot in Figure 3.2a And when the velocity is calculated from appropriate methods we get the galaxy rotation curve depicted in Figure 3.2b.

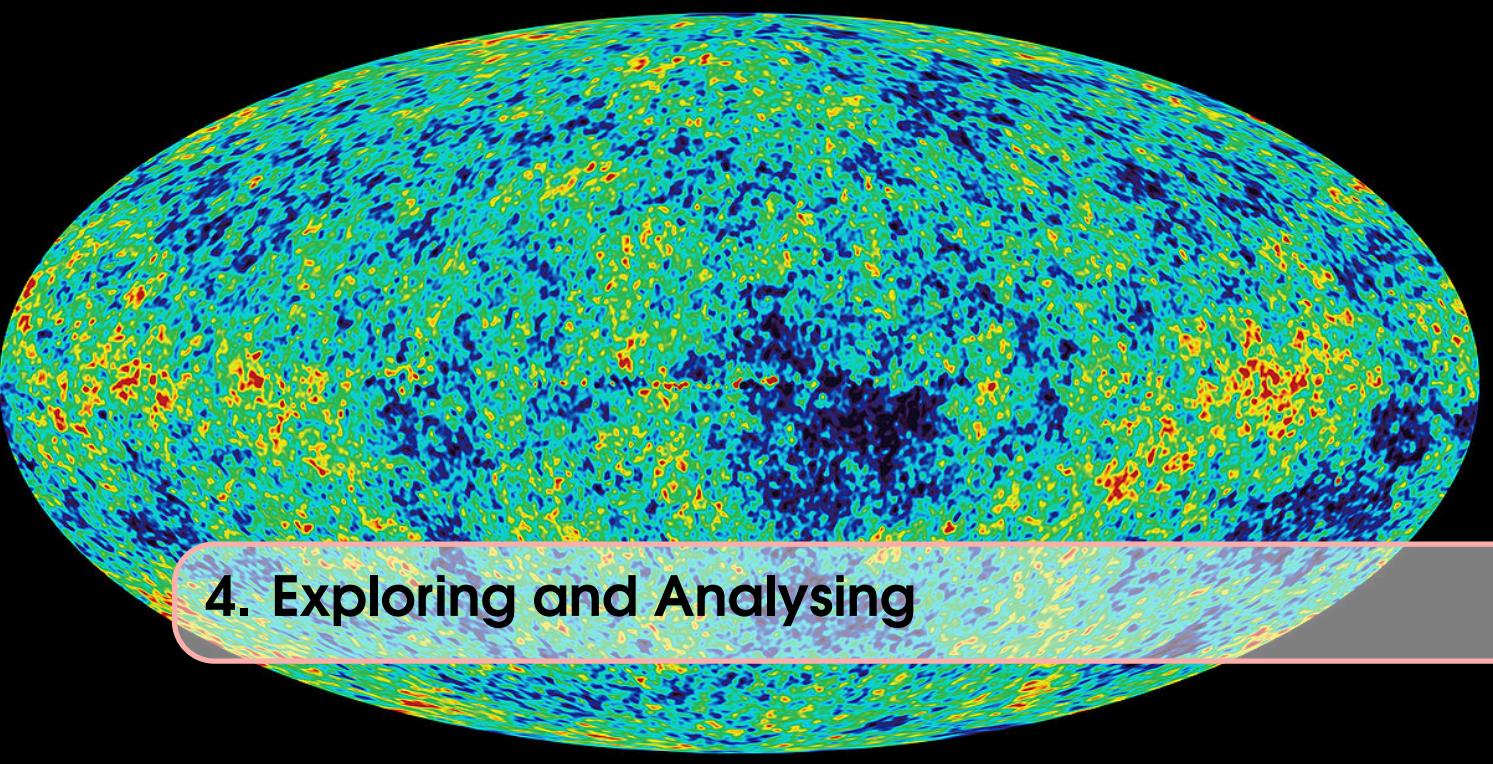
The Full code for this Activity can be found [here](#).



(a) Given Data for various distances



(b) Galaxy Rotation Curve



4. Exploring and Analysing

In this chapter, we will go through some of the basics of Data Analysis in Radio Astronomy and also some activities to help understand and grasp the topics more clearly.

4.0.1 Extracting and Working with Radio Telescope data

For any Analysis, we need some form of data and we will obtain this data from various different telescopes. We will use the site http://cutouts.cirada.ca/get_cutout/ which has multi-wavelength data. For demonstration, we will use the data of M33 (Fig 4.1) from the telescopes panSTARRS (in the visual spectrum) and VLA (in Radio Spectrum).

As we can see, the Radio image hardly shows anything. So for this demonstration, we would change our subject of interest to a galaxy with a Active

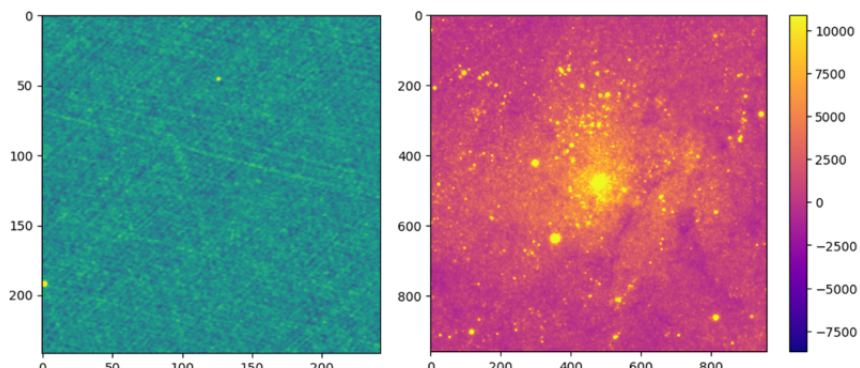


Figure 4.1: For M33 : Radio image from VLASS (on the left) and Optical Image from panSTARRS (on the right)

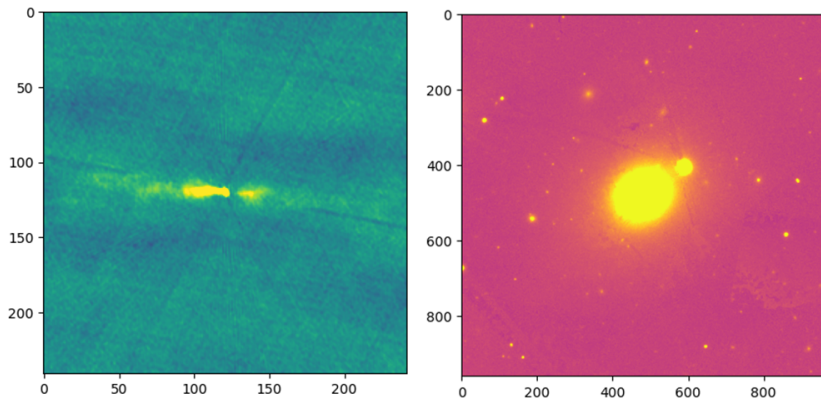


Figure 4.2: For UGC0193 : Radio image from VLASS (on the left) and Optical Image from panSTARRS (on the right)

galactic nucleus. A very good example would be UGC0193. From the images (Fig 4.2), we can clearly see the jets in the Radio image (though the optical graph is not so great to look at)

*[Code for the Data](#)

4.0.2 * Activity : CMB - a near perfect black body

Cosmic microwave background radiation (CMB) is a faint, uniform radiation that permeates the entire observable universe. It is considered the relic radiation from the Big Bang, originating approximately 13.8 billion years ago when the universe was in its infancy. The CMB is composed of photons that have cooled over time, now existing in the microwave frequency range. It provides a snapshot of the early universe, offering crucial evidence for the Big Bang theory and supporting the concept of an expanding universe.

The CMB carries valuable information about the composition, age, and structure of the cosmos, enabling scientists to study the formation of galaxies, the distribution of matter, and the seeds of cosmic structures.

In this Activity we will try to see how perfect of a black body is CMB by plotting a Black Body curve from the data (2) acquired from the COBE Satellite (10). From Fig 4.3 , We can see how perfectly the black body curve fits with our data, meaning CMB is very very near to being a perfect black body.

Also by curvefit data we can acquire the Temperature for CMB, Here it comes out to be **2.75143777 K**

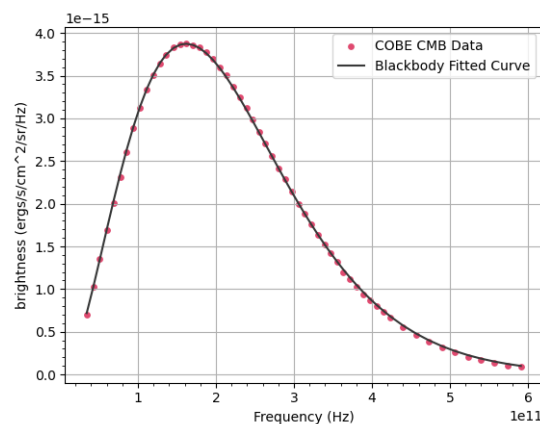


Figure 4.3: Data plotted from COBE and a curve-fit of black body curve over the data

4.1 CASA (Common Astronomy Software Applications)

CASA (Common Astronomy Software Applications) is a comprehensive software package to calibrate, image, and analyze radio astronomical data from interferometers (such as ALMA and VLA) as well as single dish telescopes. I will go on explaining CASA with the help of an example, being the **supernova remnant 3C 391**. A In-depth Tutorial can be found here (1) To save time I will be using the already calibrated data provided to us.



To start with, lets try to plot our calibrated data with UVWave on the x-axis and Amplitude on y-axis. In the CASA Terminal entering the follow code gives us the graph

```
# In CASA
plotms(vis='3c391_ctm_mosaic_spw0.ms',xaxis='uvwave',yaxis='amp',
       ydatacolumn='data', field='0', avgtime='30', correlation='RR',
       plotfile='plotms_3c391-mosaic0-uvwave.png', overwrite=True)
```

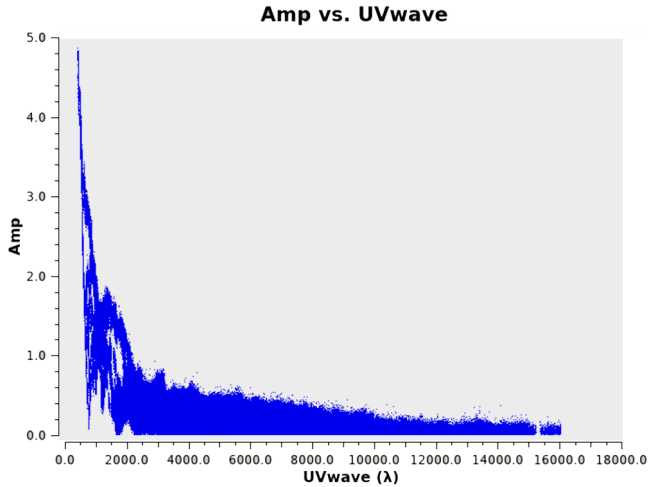


Figure 4.4: 3c391 - Amplitude vs UVWave Plot

After we have learned to visualize our data, we will look into analysing and getting some valuable information out of it.

One of the main focus in this section would be the **tclean** function CASA provides. Running the following command opens up an interactive view for us to select components or regions we are interested in

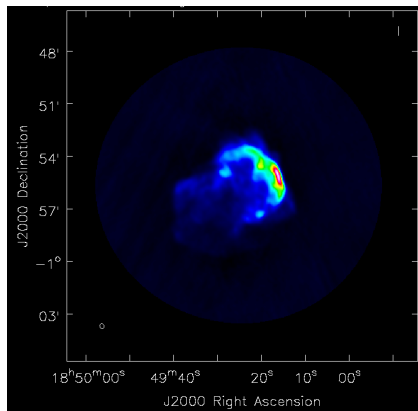
```
# In CASA
tclean(vis='3c391_ctm_mosaic_spw0.ms', imagename='3c391_ctm_spw0_multiscale',
       field='', spw='',
       specmode='mfs',
       niter=20000,
       gain=0.1, threshold='1.0mJy',
```

```
gridder='mosaic',
deconvolver='multiscale',
scales=[0, 5, 15, 45], smallscalebias=0.9,
interactive=True,
imsize=[480,480], cell=['2.5arcsec','2.5arcsec'],
stokes='I',
weighting='briggs',robust=0.5,
pbcor=False,
savemodel='modelcolumn')
```

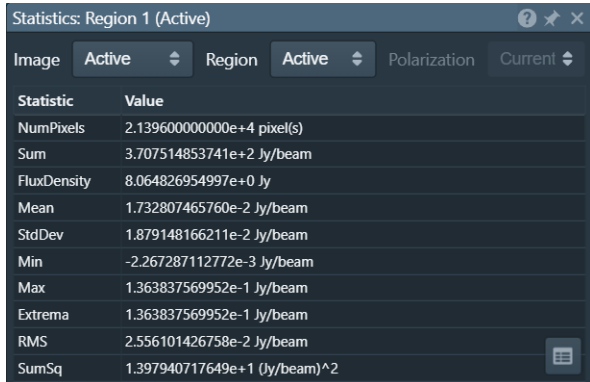
The cleaned image can be then visualised in the viewer which can be ran as follows,

```
# In CASA
viewer('3c391_ctm_spw0_multiscale.image')
```

There are multiple ways to view stats of the image, mostly it can be done with the command *imstat* in CASA. Though I like to view my images in CARTA which is an alternative to CASA and is mostly GUI based and in a sense more interactive than CASA. The following snippet shows the CARTA view of the image with all the statistics beside it. Our main focus here would be the **Flux Density** of the remnant which comes out to be around **8Jy**, we can confirm this data by comparing it to the CASA Tutorial (1)



(a) Given Data for various distances



(b) Galaxy Rotation Curve

4.2 GW170817: Merging Neutron Stars and the Dawn of Multi-Messenger Astronomy

GW170817 was a groundbreaking event in astronomy, as it marked the first simultaneous detection of gravitational waves and electromagnetic signals from the merger of two neutron stars, ushering in the era of multi-messenger astronomy. This event provided valuable insights into neutron star mergers, confirmed their association with gamma-ray bursts and kilonovae, and expanded our understanding of the universe's composition and evolution.

In this section, we will review the afterglow data for the non-thermal emission from this source that spans all frequency bands following a single spectral index of $F_\nu \propto \nu^{-0.584}$. The quantity F_ν is the flux density, which measures the amount of energy incident on the detector per unit area of the detector, an indicator of the source's brightness. A light curve is flux density represented as a function of time.

The Afterglow Data (3)

The plot below shows the VLA and Chandra Radio Telescopes data captured after the merger

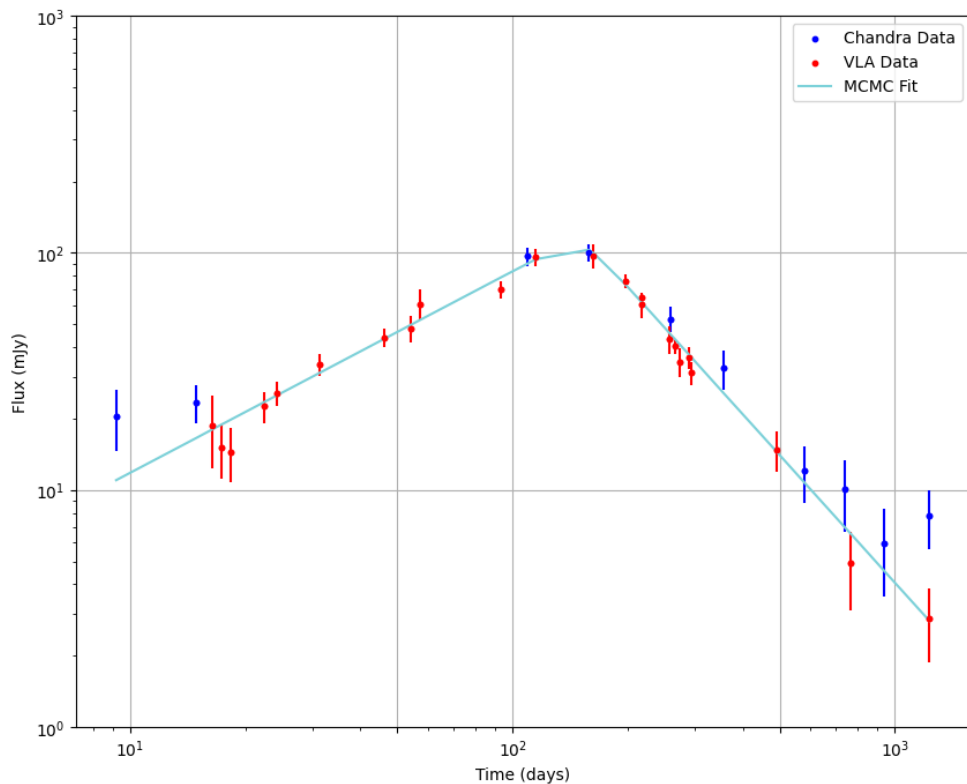


Figure 4.6: After-glow Plot from the neutron star merger event GW170817 captured by VLA (3Ghz) and Chandra

The Data has been fitted with the help of **Smooth Broken Power Law** (Given in Equation below) and **Markov Chain - Monte Carlo (MCMC)**.

$$F(t, v) = 2^{\frac{1}{s}} \left(\frac{v}{3\text{GHz}} \right)^{\beta} \cdot F_p \cdot \left[\left(\frac{t}{t_p} \right)^{-s\alpha_1} + \left(\frac{t}{t_p} \right)^{-s\alpha_2} \right]^{-\frac{1}{s}}$$

where,

F_p is the Flux Density at 3 GHz
 v is the Observing Frequency
 β is the Spectral Index
 t is the time post merger
 t_p is the light curve peak time
 s is the smoothness parameter
 α_1 and α_2 are the power-law rise and decay slopes respectively.

MCMC is a powerful computational method used for sampling complex probability distributions. It relies on the concept of Markov chains, where successive states depend only on the previous state, and randomness is introduced during the transition between states. MCMC algorithms iteratively explore the parameter space, generating a sequence of samples that approximate the desired distribution.

A Tutorial I followed for this project for MCMC (8)

The MCMC Fit seen in Figure 4.6 was made with values taken from the paper (4)

From these values we can also plot a corner plot depicting the relation between each parameters in the Smooth Broken Power law model, helping us understand it more clearly. (5)

It is important to note that the analysis made here was done with only two Telescope data and a much larger data set would give us more accurate results. One more factor that would affect the results would be how accurate we make our initials and ranges in our MCMC calculations.

Parameter	Value	Units
Broken power-law / Analytical jet model		
$F_{\nu,p}$	101 ± 3	μJy
t_p	155 ± 4	days
α_1	0.86 ± 0.04	
α_2	$-1.92^{+0.10}_{-0.12}$	
$\log_{10}(s)$	$0.56^{+0.12}_{-0.11}$	
β	-0.584 ± 0.002	
χ^2/dof	75/97	
p	2.168 ± 0.004	
E/n_{ISM}	$\simeq 1.5 \times 10^{53}$	erg cm^3
θ_v	$\simeq 14 - 20$	degrees
θ_j	$\simeq 1 - 4$	degrees
Structured jet model		
θ_v	35.2 ± 0.6	degrees
ϵ_e	$7.8^{+1.0}_{-0.6} \times 10^{-3}$	
ϵ_b	$9.9^{+4.7}_{-2.2} \times 10^{-4}$	
p	$2.07^{+0.01}_{-0.02}$	
n_{ISM}	$9.8^{+0.2}_{-1.6} \times 10^{-3}$	cm^{-3}
χ^2/dof	95.2/97	

Figure 4.7: Reference MCMC Fit Values for GW170817 merger(4)

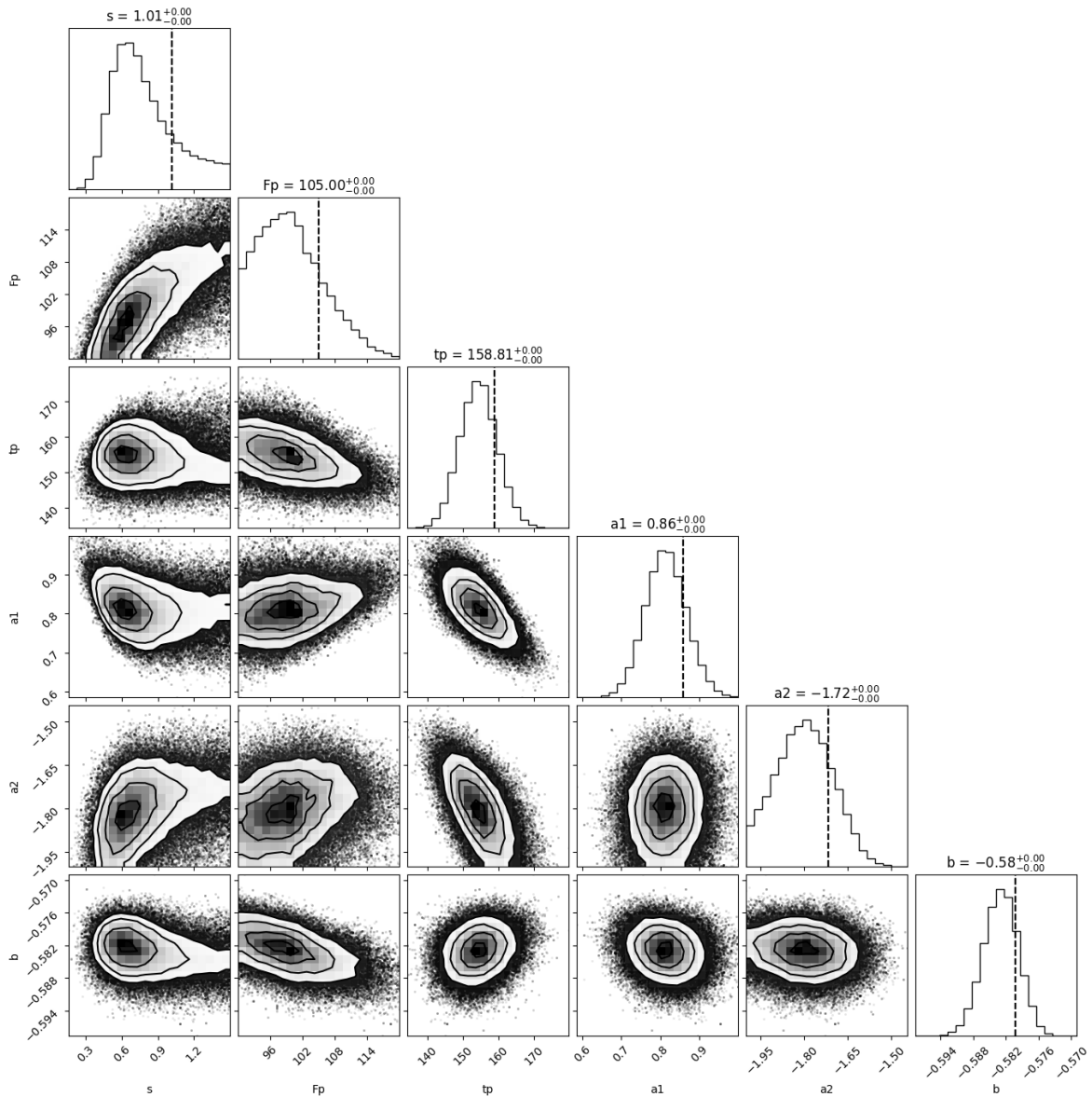


Figure 4.8: Corner plot showing the relation between different parameters.

4.3 Fast Radio Bursts: Analysing Pulsar and its Dispersion Measure

The discovery of radio pulsars over a half century ago was a seminal moment in astronomy. It demonstrated the existence of neutron stars, gave a powerful observational tool to study them, and has allowed us to probe strong gravity, dense matter, and the interstellar medium. More recently, pulsar surveys have led to the serendipitous discovery of fast radio bursts (FRBs). While FRBs appear similar to the individual pulses from pulsars, their large dispersive delays suggest that they originate from far outside the Milky Way and hence are many orders-of-magnitude more luminous. While most FRBs appear to be one-off, perhaps cataclysmic events, two sources are now known to repeat and thus clearly have a longer lived central engine.

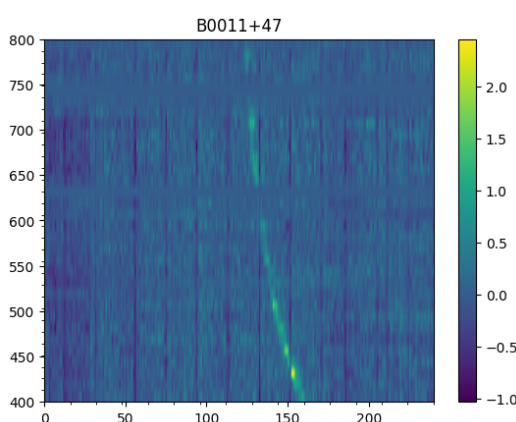
(7)

In this section we will go through some Pulsar Data analysing its Frequency and calculating proper Dispersion Measure for it

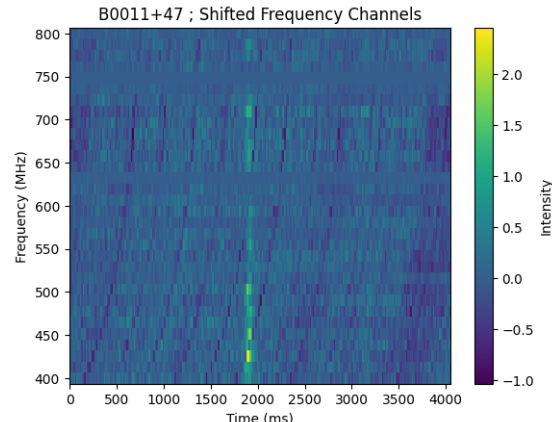
To Elaborate on Dispersion Measure, is itself observationally as a broadening of an otherwise sharp pulse when a pulsar is observed over a finite bandwidth. Technically the DM is the “integrated column density of free electrons between an observer and a pulsar”. It is perhaps easier to think about dispersion measure representing the number of free electrons between us and the pulsar per unit area. So if we could construct a long tube of cross-sectional area 1 square cm and extending from us to the pulsar, the DM would be proportional to the number of free electrons inside this volume.(11)

The Data can be found here.(12)

And the Code for this can be found here (9)



(a) Waterfall plot for given Pulsar data



(b) Aligned Waterfall plot for the same data

We need to align the Frequency channels in order to add up the pulse-lines cause they experience a Time-delay during the observation.

Once this is done we can finally calculate the Dispersion-Measure. We do this by first calculating the Time-Series by summing up all the frequency channels. After this we define Signal-to-Noise Ratio (SNR) by taking the ratio of maximum to average value of Time series.

A Time-Series vs Time plot can be seen in Figure 4.10

Now to Measure the Dispersion Measure for the Pulsar we select the highest SNR value.

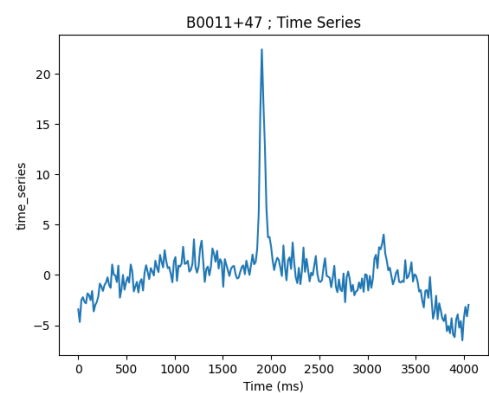


Figure 4.10: Time series vs time(ms) plot for the pulsar data

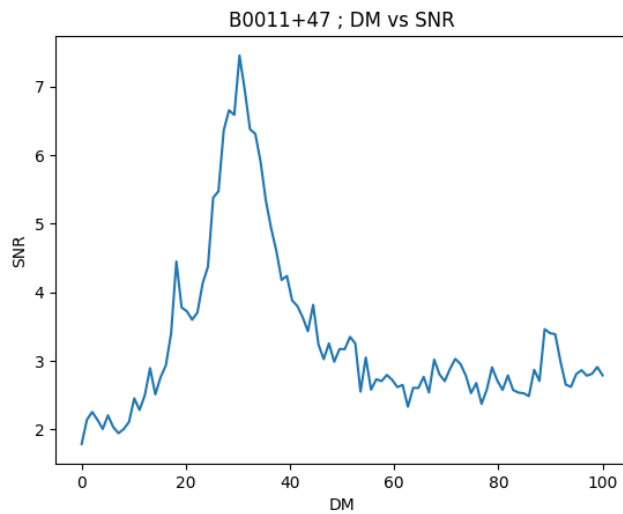


Figure 4.11: DM vs SNR plot where we can see a nice maximum peak for SNR

This is where we get a Peak in the Time series
plot 4.10

From Figure 4.11 we can calculate the DM
value to be around **30.30**.



Bibliography

- (CAS) CASA. *VLA Continuum Tutorial 3C391-CASA6.4.1*. https://casaguides.nrao.edu/index.php?title=VLA_Continuum_Tutorial_3C391-CASA6.4.1 (cited on pages 19, 20).
- (COB) COBE. *Cobe Data*. https://github.com/Drosophilaa/KSP-Radio/blob/main/Assign2/COBE_CMB_data.txt (cited on page 18).
- (kmo) kmooley. *GW170817 Afterglow Data*. https://github.com/kmooley/GW170817/blob/main/gw170817_afterglow_data_full.txt (cited on page 21).
- (Mak+21a) S. Makhathini et al. "The Panchromatic Afterglow of GW170817: The Full Uniform Data Set, Modeling, Comparison with Previous Results, and Implications". In: *The Astrophysical Journal* 922.2 (Nov. 2021), page 154. DOI: 10.3847/1538-4357/ac1ffc. URL: <https://doi.org/10.3847%2F1538-4357%2Fac1ffc> (cited on page 22).
- (Mak+21b) Sphesihle Makhathini et al. "The panchromatic afterglow of GW170817: the full uniform data set, modeling, comparison with previous results, and implications". In: *The Astrophysical Journal* 922.2 (2021), page 154 (cited on page 22).
- (MSK15) J.M. Marr, R.L. Snell, and S.E. Kurtz. *Fundamentals of Radio Astronomy: Observational Methods*. Series in Astronomy and Astrophysics. CRC Press, 2015. ISBN: 9781498770194. URL: <https://books.google.co.in/books?id=T54oCwAAQBAJ> (cited on pages 6, 7, 11, 12).
- (PHL19) E. Petroff, J. W. T. Hessels, and D. R. Lorimer. "Fast radio bursts". In: *The Astronomy and Astrophysics Review* 27.1 (May 2019). DOI:

- 10 . 1007 / s00159 - 019 - 0116 - 6. URL: <https://doi.org/10.1007%2Fs00159-019-0116-6> (cited on page 24).
- (pra) prappleizer. *Markov-Chain Monte Carlo Tutorial*. https://prappleizer.github.io/Tutorials/MCMC/MCMC_Tutorial_Solution.html (cited on page 22).
- (Sel) Self. *FRB:Pulsar Code*. <https://github.com/Drosophilaa/KSP-Radio/blob/main/Assign4/main.ipynb> (cited on page 24).
- (Unka) Unknown. *Cobe Info*. <https://ui.adsabs.harvard.edu/abs/1990ApJ...354L..37M/abstract> (cited on page 18).
- (Unkb) Unknown. *DM Info*. <https://astronomy.swin.edu.au/cosmos/p/pulsar+dispersion+measure> (cited on page 24).
- (Unkc) Unknown. *FRB:Pulsar Data*. https://github.com/Drosophilaa/KSP-Radio/blob/main/Assign4/final_pulsar_data.npy (cited on page 24).
- (Unkd) Unknown. *Synthetic Spectral Data*. https://github.com/Drosophilaa/KSP-Radio/tree/main/Assign2/galaxy_21cm_spectrum (cited on page 14).
- (Wik) Wikipedia. *21cm Hydrogen Line*. https://en.wikipedia.org/wiki/Hydrogen_line#/media/File:Hydrogen-SpinFlip.svg (cited on page 14).